Helical Structures

Deutsche Ausgabe: DOI: 10.1002/ange.201510140
Internationale Ausgabe: DOI: 10.1002/anie.201510140

Inversion of the Supramolecular Chirality of Nanofibrous Structures through Co-Assembly with Achiral Molecules

Guo-Feng Liu[+], Ling-Yun Zhu[+], Wei Ji, Chuan-Liang Feng, and Zhi-Xiang Wei*

Abstract: *To understand the behavior of chiral nanostructures, it is of critical importance to study how achiral molecules regulate the chirality of such nanostructures and what the main driving forces for the regulation processes are. In this work, the supramolecular chirality of helical nanofibers consisting of phenylalanine-based enantiomers is inverted by achiral bis-(pyridinyl) derivatives through co-assembly. This inversion is mainly mediated by intermolecular hydrogen bonding interactions between the achiral additives and the chiral molecules, which may induce stereoselective interactions and different reorientations for the assembled molecules, as confirmed by calculations. This work not only exemplifies a feasible method to invert the helicity of chiral nanostructures by the addition of achiral molecules, but also provides a method to explore their functions in environments where chiral and achiral molecules are in close proximity.*

Helical and twisted nanostructures with controllable chirality are attracting attention owing to their crucial roles in the fields of catalysis,[1] sensing or recognition,[2] chiroptical switches,[3] medicine,[4] biomineralization,[5] and biology.[6] To tune the chirality of nanostructures and to influence the conformation of chiral assemblies, the participation of chiral guests or asymmetric factors is usually required.[7] On the other hand, it has remained challenging to tune the chiral conformation (right-handed, *P*; left-handed, *M*) of nanostructures by achiral molecules, but it is very important to have an overall understanding of the assembly mechanisms of chiral nanostructures in materials science and biology.[8] Such studies should provide complementary information on regulating the chirality of nanostructures and methods for exploring their functions when in close proximity with achiral molecules.

To obtain chiral nanostructures, supramolecular assemblies are often employed as they may self-assemble in a controllable way through non-covalent interactions, such as hydrogen bonding, π–π stacking, and electrostatic interactions.[9] The chirality of supramolecular nanostructures is usually determined by the molecular chirality.[10] Because of the non-covalent interactions, some chiral nanostructures are successfully controlled by external stimuli, such as light,[11] temperature,[12] solvent,[13] pH,[14] rotary stirring,[15] and chiral additives,[16] leading to a so-called helix-to-helix transition between *P* and *M*. However, in these cases, chiral guests or asymmetric factors are always present. In fact, chiral supramolecular structures usually do not exist alone in biological or self-assembled aggregates, but are closely dependent on the guests around them, which can be chiral, asymmetric, or achiral. However, little is known about the helical inversion of supramolecular nanostructures triggered by achiral molecules, which is very important for understanding the origins of chirality in supramolecular systems.

Inspired by the above situation, we selected phenylalanine-based enantiomers (right-handed DPF and left-handed LPF, Scheme 1) as basic units for constructing supramolecular chiral nanostructures. Two achiral bis(pyridinyl) derivatives (BPy1 and BPy2) with different chemical structures were employed to regulate the chirality of the nanostructures. The handedness of the nanostructures could be inverted simply by exchanging the achiral molecule (Scheme 1). This process was shown to be mainly mediated by intermolecular hydrogen bonding interactions between the achiral molecules and the enantiomers during co-assembly,

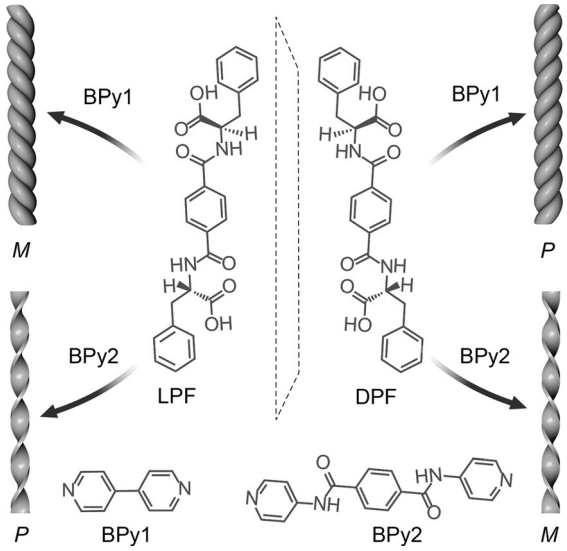

Scheme 1. Helical inversion of the nanofibers. *M* and *P* denote left- and right-handed helical or twisted nanofibers, respectively. LPF and DPF are enantiomeric gelators. BPy1 and BPy2 are achiral bis(pyridinyl) derivatives.

[*] G. F. Liu,[+] W. Ji, Prof. C. L. Feng
State Key Lab of Metal Matrix Composites
School of Materials Science and Engineering
Shanghai Jiao Tong University
Shanghai 200240 (China)
E-mail: clfeng@sjtu.edu.cn
Dr. L. Y. Zhu,[+] Prof. Z. X. Wei
Key Laboratory of Nanosystem and Hierarchical Fabrication
National Center for Nanoscience and Technology
Beijing 100190 (China)
[+] These authors contributed equally to this work.

Supporting information for this article is available on the WWW under http://dx.doi.org/10.1002/anie.201510140.

which can further induce different rearrangements and assemblies.

The syntheses of DPF, LPF, and BPy2 are outlined in the Supporting Information,[17] and BPy1 is commercially available. Both DPF and LPF self-assembled into transparent nanofibrous hydrogels in aqueous solution (Supporting Information, Figure S1 and S2). However, the formed hydrogels were unstable and decomposed within twelve hours. An equimolar amount of a bis(pyridinyl) derivative (BPy1 or BPy2) was then mixed with DPF or LPF. The co-assembled hydrogels were obtained by a heating and cooling process (Figure S1). Compared with the DPF and LPF hydrogels, the co-assembled hydrogels, DPF–BPy1 and LPF–BPy1, were much more stable for a longer period of time (Figure S1). This was further confirmed by rheology measurements, as the storage (G') and loss moduli (G'') of the co-assembled hydrogels were higher than those of the DPF and LPF hydrogels (Figures S3–S5). Typically, greater G' and G'' values were observed for the LPF–BPy1 and LPF–BPy2 hydrogels, suggesting that the achiral molecules formed more stable assembled structures with LPF than with DPF. Furthermore, higher G' and G'' values were also observed with BPy2 compared with BPy1. This may be due to the fact that BPy2 can interact through two additional amide–amide hydrogen bonds, indicating that the amide groups of the achiral molecule play an important role in rendering the co-assembly of BPy2 and LPF or DPF more stable and in determining the rheological properties of the hydrogels. All of these results imply that the hydrogels formed by the co-assembly of the LPF/DPF enantiomers and the achiral compounds and their rheological properties depend on both the molecular chirality and the structure of the achiral molecule.

The nanofibrous structures of the co-assembled hydrogels were imaged by scanning electron microscopy (SEM; Figure 1). An equimolar mixture of DPF and BPy1 (DPF–BPy1) formed right-handed (*P*) helical fibers (Figure 1a), whereas an equimolar mixture of LPF and BPy1 (LPF–BPy1) co-assembled into left-handed (*M*) helical nanofibers (Figure 1b). Furthermore, whereas LPF and BPy2 assembled into right-handed twisted nanoribbons (Figure 1c), the DPF–BPy2 nanofibers were formed as left-handed twisted nanoribbons (Figure 1d). These results suggest that nanoscale twists of opposite handedness could be generated from the same chiral molecule. This chiral inversion was obviously triggered by achiral BPy1 and BPy2, which differs from previous approaches.[11–16] These results were consistently obtained in several experiments.

To gain further insight, the hydrogels were analyzed by CD spectroscopy. For the DPF hydrogels, significant positive Cotton effects were observed at 210 nm and 268 nm, whereas the LPF hydrogels exhibited negative Cotton effects at 210 nm and 268 nm (Figure S6). Similarly, positive Cotton effects (210 nm and 268 nm) were observed for the DPF–BPy1 hydrogel and negative Cotton effects for the LPF–BPy1 hydrogel (Figure 2a). Interestingly, for the DPF–BPy2 hydrogel, the CD spectrum exhibited a positive Cotton effect at 210 nm and a negative Cotton peak at 268 nm (Figure 2b). Compared with DPF–BPy1, a chiral transition into the opposite optically active hydrogel was achieved only by exchanging the achiral additive (BPy1 and BPy2), which is in good agreement with the SEM results. Thus a relationship between the handedness of the helical fibers and the CD signs could be established. The right-handed (*P*) DPF–BPy1 nanofibers exhibited a positive Cotton effect at 268 nm, whereas left-handed (*M*) LPF–BPy1 fibers showed a negative Cotton effect at 268 nm (Figure 2a). In contrast, *P*-twisted LPF–BPy2 nanoribbons exhibited a positive Cotton effect at 268 nm (Figure 2a), and *M*-twisted DPF–Bpy2 nanoribbons showed a negative Cotton effect at the same wavelength (Figure 2b). It must be pointed out that the left-handed nanofibers and right-handed nanoribbons are not exactly

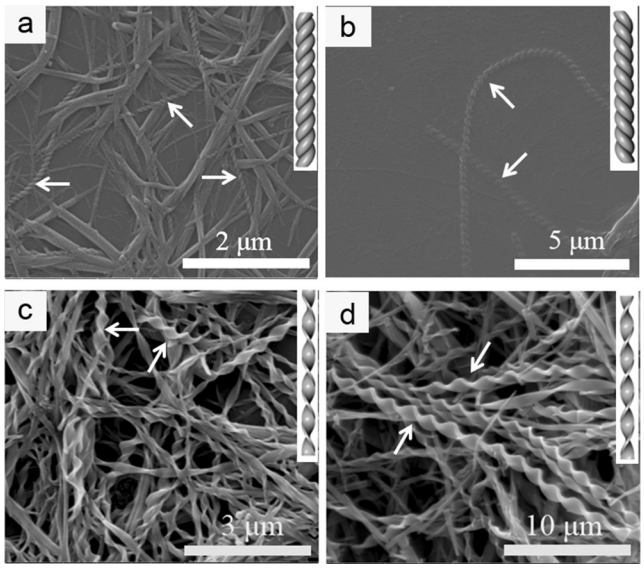

Figure 1. SEM images of a) right-handed helical fibers in the DPF–BPy1 xerogel, b) left-handed helical fibers in the LPF–BPy1 xerogel, c) left-handed helical fibers in the DPF–BPy2 xerogel, and d) right-handed helical fibers in the LPF–BPy2 xerogel.

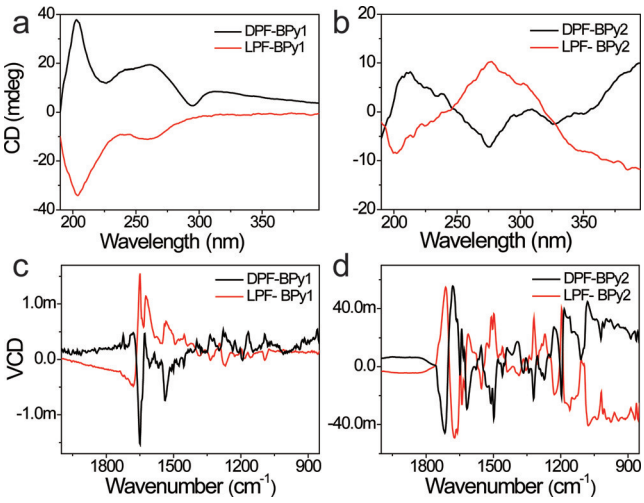

Figure 2. CD and VCD spectra of the DPF–BPy1 (a), LPF–BPy1 (c), DPF–BPy2 (b), and LPF–BPy2 (d) hydrogels were obtained by using a 0.1 mm quartz cuvette with a total gelator concentration of 2.0 mg mL^{-1}.

enantiomers, and their CD spectra should not be exact mirror images. In both cases, the chirality of the supramolecular nanostructures was successfully inverted by exchanging the achiral additive (BPy1 vs. BPy2).

The optical activity and the chirality of these hydrogels were investigated by vibrational circular dichroism (VCD) spectroscopy. For the LPF hydrogels, the C=O stretching band exhibited a negative VCD signal at 1800–1700 cm^{-1} and a negative VCD signal at 1700–1620 cm^{-1} (Figure S7). On the other hand, the signs of both of these VCD bands were positive for the DPF hydrogels (Figure S7). The VCD spectra of DPF and LPF were almost mirror images of each other. Similarly, the VCD spectrum of LPF–BPy1 showed a negative VCD signal at 1800–1700 cm^{-1} and a positive one at 1700–1600 cm^{-1} (Figure 2c). The DPF–BPy1 hydrogel resulted in a positive VCD signal at 1800–1700 cm^{-1} and a negative one at 1700–1600 cm^{-1} (Figure 2c). Surprisingly, the C=O stretching band of the LPF–BPy2 hydrogel showed a significant positive VCD band at 1800–1700 cm^{-1} and a negative VCD signal at 1700–1600 cm^{-1}. For DPF–BPy2, however, the signs of the VCD bands at 1800–1700 cm^{-1} and 1700–1600 cm^{-1} were negative and positive, respectively (Figure 2d). As discussed above, the observed chiral and morphological transformations of the hydrogel nanostructures should be attributed to the presence of achiral additives, which leads to supramolecular chirality inversion and chiroptical inversion.

To understand the arrangement of molecular aggregates in the co-assembled hydrogels, colorless cocrystals of LPF–BPy1 were crystallized from tetrahydrofuran/*para*-xylene (3:5, v/v) solution. Detailed crystallographic data can be found in Table S2. The crystal structure and packing diagram of LPF–BPy1 suggested that the main driving force for the co-assembly was the formation of two types of intermolecular hydrogen bonds (C–N···H–O and N–H···O=C; Figure 3). First, one-dimensional (1D) self-assembly in a head-to-tail fashion occurred through the formation of hydrogen bonds (bond length: 1.76 Å) between a pyridyl nitrogen atom and the HO group of a carboxylic acid (H···N, Table S2). Second, three-dimensional (3D) crystal networks were obtained through the formation of hydrogen bonds between an amide N–H group and a carboxylic acid C=O moiety (2.10 Å, H···O, Table S2). These two kinds of intermolecular hydrogen bonds thus are the main driving force for stabilizing the cocrystal framework (Figure 3).

To simulate the chiroptical inversion phenomena of the molecular aggregates, ab initio calculations were performed within the framework of density functional theory (DFT) with the B3LYP functional, Grimme's dispersion correction (B3LYP-D), and the 6-31G(d,p) basis set. Here, we focus only on the properties of LPF as the experimental CD spectra of LPF and DPF are almost mirror images of each other. The experimental crystal structure of (*M*)-LPF showed that two molecules were nearly perpendicular to each other, and the two terminal phenyl groups were arranged in a *trans* fashion (Figure 4a). However, in the B3LYP-D/6-31G (d,p) optimized structure of the (*P*)-LPF dimer, one molecule was nearly parallel to the other one, with the smallest intermolecular distance being approximately 3.2 Å, and the two terminal phenyl groups are *cis* to each other (Figure 4b).

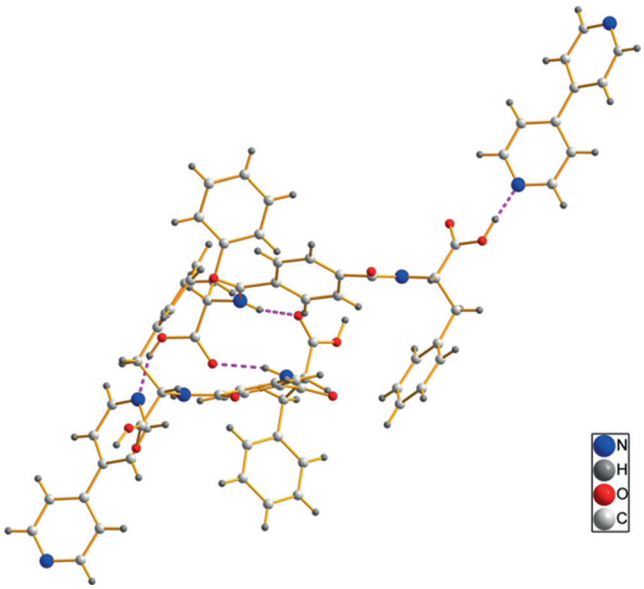

Figure 3. The packing structure of LPF–BPy1 stabilized by hydrogen bonds (pink dashed lines) in the cocrystal state.

Based on the experimental crystal structure and the optimized geometry, time-dependent density functional theory (TDDFT) calculations with the long-range-corrected (LRC) functional ωB97x and the 6-31G(d,p) basis set were conducted to calculate the CD spectra of the co-assembly. For the dimer (*M*)-LPF, two negative peaks A and B were found between 190 and 400 nm (Figure 4). Peak A is located at approximately 243 nm, corresponding to the S8 and S10

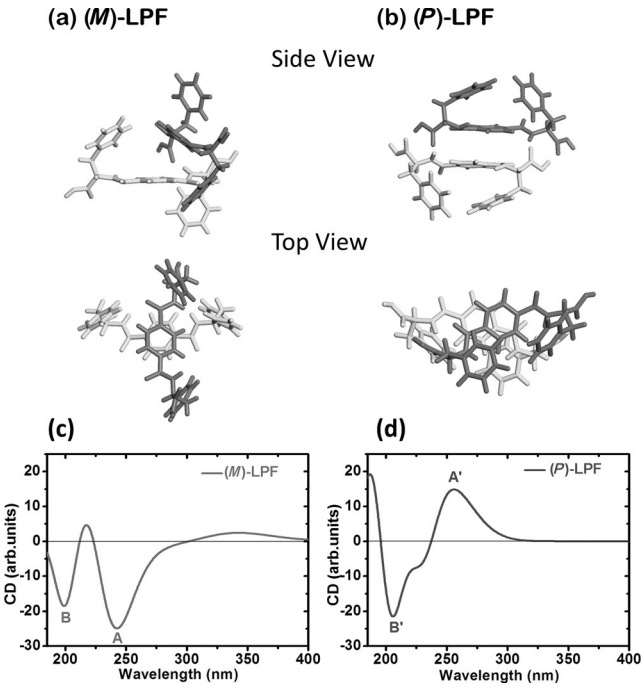

Figure 4. a) Structure of the (*M*)-LPF dimer determined by crystal-structure analysis. b) B3LYP-D/6-31G (d,p) optimized geometry of the (*P*)-LPF dimer. c,d) TDDFT calculated CD spectra of the two dimers at the ωB97x/6-31G (d,p) level of theory.

excited states (see Table S3), which are associated with intramolecular transitions from the amide linkage to the central aryl group (see Figure S8a). Peak B is located at 200 nm and due to contributions from the S34 and S35 excited states, which are associated with intramolecular $\pi\rightarrow\pi^*$ transitions in the terminal phenyl group of one molecule and intermolecular transitions from the amide linkage of one molecule to the central aryl group of another molecule (see Figure S8a).

However, for the dimer (*P*)-LPF, in contrast to (*M*)-LPF, one positive peak, A′, at approximately 256 nm and one negative peak, B′, at about 206 nm were found between 190–400 nm. Natural transition orbital (NTO) analysis showed that peak A′ is mainly due to intermolecular $\pi\rightarrow\pi^*$ transitions of the central aryl group, and peak B′ is associated with transitions at the central aryl group and transitions from the amide linkage or a terminal phenyl group to the central aryl group (see Figure S8b). These two peaks are mainly due to the exciton coupling of two molecules. The experimental CD spectra, including the signs and shapes of the bands, were well reproduced by our calculations. Our calculations thus fully support the experimentally observed chiroptical inversion phenomena.

Whereas BPy1 has only one kind of hydrogen-bonding site (pyridine), BPy2 has two kinds of binding sites (pyridine and amide), which leads to different interaction modes with DPF and LPF. Typically, there is competition between the COOH/pyridine and amide/amide groups of the achiral and chiral compounds. BPy1 should interact with both DPF and LPF via the COOH sites, whereas BPy2 interacts with them through both the COOH and amide groups. These two interactions lead to a parallel arrangement, which could possibly cause the chirality inversion. Therefore, different chirality phenomena can be expected for further achiral additives, which could be obtained by varying the amide group, for example, and more useful information on chirality regulation by achiral molecules should be obtainable. Such studies are currently in progress in our group.

In summary, the supramolecular chirality of nanofibrous structures has been inverted by the addition of different achiral molecules and the formation of intermolecular hydrogen bonds between these additives and the supramolecules, which induce stereoselective interactions and different reorientations. This system is one of very few examples where achiral molecules have been shown to trigger chirality inversions of nanostructures through co-assembly with chiral compounds. It exemplifies a feasible shortcut to achieve helical inversions by rationally designing basic molecular structures. This method can be applied in complementary studies on regulating the chirality of nanostructures and for exploring their role in environments where chiral and achiral molecules are in close proximity, for example, in biological or self-assembled aggregates.[18]

Acknowledgements

We thank the NSFC (51573092, 51273111, 51173105), the National Basic Research Program of China (973 Program, 2012CB933803), and the SJTU-UM Collaborative Research Program for Professors of Special Appointment (Eastern Scholar) at the Shanghai Institutions of Higher Learning.

Keywords: chirality · co-assembly · helical structures · hydrogels · supramolecular chemistry

How to cite: *Angew. Chem. Int. Ed.* **2016**, *55*, 2411–2415
Angew. Chem. **2016**, *128*, 2457–2461

[1] a) I. Sato, K. Kadowaki, H. Urabe, Y. Ono, S. Shinkai, J. H. Jung, K. Soaia, *Tetrahedron Lett.* **2003**, *44*, 721–724; b) F. Rodríguez-Llansola, B. Escuder, J. F. Miravet, *J. Am. Chem. Soc.* **2009**, *131*, 11478–11484.

[2] a) J. J. L. M. Cornelissen, A. E. Rowan, R. J. M. Nolte, N. A. J. M. Sommerdijk, *Chem. Rev.* **2001**, *101*, 4039–4070; b) J. L. Schaefer, S. S. Moganty, D. A. Yanga, L. A. Archer, *J. Mater. Chem.* **2011**, *21*, 10094–10101; c) W. Edwards, D. K. Smith, *J. Am. Chem. Soc.* **2014**, *136*, 1116–1124.

[3] a) J. J. D. de Jong, L. N. Lucas, R. M. Kellogg, J. H. van Esch, B. L. Feringa, *Science* **2004**, *304*, 278–281; b) C. F. J. Faul, *Acc. Chem. Res.* **2014**, *47*, 3428–3438; c) G. Echue, G. C. Lloyd-Jones, C. F. J. Faul, *Chem. Eur. J.* **2015**, *21*, 5118–5128; d) R. Ahmed, S. K. Patra, I. W. Hamley, I. Manners, C. F. J. Faul, *J. Am. Chem. Soc.* **2013**, *135*, 2055–2058; e) R. Wang, J. Zhang, X. H. Wan, *Chem. Rec.* **2015**, *15*, 475–494; f) H. B. Wei, N. Shi, J. L. Zhang, Y. Guan, J. Zhang, X. H. Wan, *Chem. Commun.* **2014**, *50*, 9333–9335; g) R. Wang, X. F. Li, J. W. Bai, J. Zhang, A. H. Liu, X. H. Wan, *Macromolecules* **2015**, *48*, 1553–1562.

[4] a) G. L. Liang, Z. M. Yang, R. J. Zhang, L. H. Li, Y. J. Fan, Y. Kuang, Y. Gao, T. Wang, W. W. Lu, B. Xu, *Langmuir* **2009**, *25*, 8419–8422; b) J. Li, Y. Kuang, Y. Gao, X. Du, J. Shi, B. Xu, *J. Am. Chem. Soc.* **2012**, *134*, 542–545.

[5] a) S. Kobayashi, N. Hamasaki, M. Suzuki, M. Kimura, H. Shirai, K. Hanabusa, *J. Am. Chem. Soc.* **2002**, *124*, 6550–6551; b) Y. O. Jong, H. Jung, K. Hanabusa, S. Shinkai, *J. Am. Chem. Soc.* **2000**, *122*, 5008–5009; c) H. K. Jong, H. Jung, M. Masuda, T. Shimizu, S. Shinkai, *J. Am. Chem. Soc.* **2001**, *123*, 8785–8789.

[6] G. F. Liu, D. Zhang, C. L. Feng, *Angew. Chem. Int. Ed.* **2014**, *53*, 7789–7793; *Angew. Chem.* **2014**, *126*, 7923–7927.

[7] a) J. van Gestel, A. R. A. Palmans, B. Titulaer, J. A. J. M. Vekemans, E. W. Meijer, *J. Am. Chem. Soc.* **2005**, *127*, 5490–5494; b) J. H. K. K. Hirschberg, L. Brunsveld, A. Ramzi, J. A. J. M. Vekemans, R. P. Sijbesma, E. W. Meijer, *Nature* **2000**, *407*, 167–170; c) E. Yashima, K. Maeda, *Macromolecules* **2007**, *40*, 3–12; d) E. Yashima, Y. Maeda, Y. Okamoto, *J. Am. Chem. Soc.* **1998**, *120*, 8895–8896; e) K. Morino, K. Maeda, E. Yashima, *Macromolecules* **2003**, *36*, 1480–1486; f) W. Makiguchi, S. Kobayashi, Y. Furusho, E. Yashima, *Angew. Chem. Int. Ed.* **2013**, *52*, 5275–5279; *Angew. Chem.* **2013**, *125*, 5383–5387; g) D. K. Smith, *Chem. Soc. Rev.* **2009**, *38*, 684–694; h) T. Gibaud, E. Barry, M. J. Zakhary, M. Henglin, A. Ward, Y. Yang, C. Berciu, R. Oldenbourg, M. F. Hagan, D. Nicastro, R. B. Meyer, Z. Dogic, *Nature* **2012**, *481*, 348–351; i) X. Wu, Y. Li, B. Li, X. Zhu, K. Hanabusa, Y. Yang, *J. Am. Chem. Soc.* **2009**, *131*, 5986–5993; j) M. S. Spector, J. V. Selinger, J. M. Schnur in *Materials-Chirality*, Wiley, New York, **2004**, pp. 281–372; k) T. Koga, M. Matsuoka, N. Higashi, *J. Am. Chem. Soc.* **2005**, *127*, 17596–17597; l) L. V. Joël, J. E. Moreau, M. Wong, C. Man, C. Bied, *J. Am. Chem. Soc.* **2001**, *123*, 1509–1510.

[8] a) E. Yashima, K. Maeda, Y. Okamoto, *Nature* **1999**, *399*, 449–451; b) S. Yamamoto, H. Iida, E. Yashima, *Angew. Chem. Int. Ed.* **2013**, *52*, 6849–6853; *Angew. Chem.* **2013**, *125*, 6987–6991; c) M. Ikeda, Y. Tanaka, T. Hasegawa, Y. Furusho, E. Yashima, *J. Am. Chem. Soc.* **2006**, *128*, 6806–6807; d) N. Pa, H. Ro, *Mol. Cell. Biol.* **1987**, *7*, 4297; e) W. D. Staatz, K. F. Fok, M. M. Zutter,

S. P. Adams, B. A. Rodriguez, S. A. Santoro, *J. Biol. Chem.* **1991**, *266*, 7363; f) B. E. Vogel, S. J. Lee, A. Hildebrand, W. Craig, M. D. Pierschbacher, F. Wong-Staal, E. Ruoslahti, *J. Cell Biol.* **1993**, *121*, 461.

[9] a) Y. Rong, P. Chen, D. Wang, M. Liu, *Langmuir* **2012**, *28*, 6356 – 6363; b) Q. Jin, L. Zhang, X. Zhu, P. Duan, M. Liu, *Chem. Eur. J.* **2012**, *18*, 4916 – 4922; c) Z. Shen, T. Wang, M. Liu, *Chem. Commun.* **2014**, *50*, 2096 – 2099; d) Z. Shen, T. Wang, M. Liu, *Angew. Chem. Int. Ed.* **2014**, *53*, 13424 – 13428; *Angew. Chem.* **2014**, *126*, 13642 – 13646; e) L. Zhang, X. Wang, T. Wang, M. Liu, *Small* **2015**, *11*, 1025 – 1038; f) B. Adhikari, J. Nanda, A. Banerjee, *Soft Matter* **2011**, *7*, 8913 – 8922; g) T. Tu, W. Fang, X. Bao, X. Li, K. H. Dötz, *Angew. Chem. Int. Ed.* **2011**, *50*, 6601 – 6605; *Angew. Chem.* **2011**, *123*, 6731 – 6735; h) L. Frkanec, M. Zinic, *Chem. Commun.* **2010**, *46*, 522 – 537; i) T. Baumberger, C. Caroli, D. Martina, *Nat. Mater.* **2006**, *5*, 552 – 555.

[10] a) F. J. M. Hoeben, P. Jonkheijm, E. W. Meijer, A. P. H. J. Schenning, *Chem. Rev.* **2005**, *105*, 1491 – 1546; b) C. C. Lee, C. Grenier, E. W. Meijer, A. P. H. J. Schenning, *Chem. Soc. Rev.* **2009**, *38*, 671 – 683; c) D. Pijper, B. L. Feringa, *Soft Matter* **2008**, *4*, 1349 – 1372.

[11] Q. Li, L. Green, N. Venkataraman, I. Shiyanovskaya, A. Khan, A. Urbas, J. W. Doane, *J. Am. Chem. Soc.* **2007**, *129*, 12908 – 12909.

[12] a) A. Brizard, C. Aimé, T. Labrot, I. Huc, D. Berthier, F. Artzner, B. Desbat, R. Oda, *J. Am. Chem. Soc.* **2007**, *129*, 3754 – 3762; b) K. Nagai, K. Maeda, Y. Takeyama, T. Sato, E. Yashima, *Chem. Asian J.* **2007**, *2*, 1314 – 1321; c) M. Fujiki, *J. Am. Chem. Soc.* **2000**, *122*, 3336 – 3343.

[13] a) R. S. Johnson, T. Yamazaki, A. Kovalenko, H. Fenniri, *J. Am. Chem. Soc.* **2007**, *129*, 5735 – 5743; b) S. I. Sakurai, K. Okoshi, J. Kumaki, E. Yashima, *J. Am. Chem. Soc.* **2006**, *128*, 5650 – 5651; c) P. A. Underwood, F. A. Bennett, A. Kirkpatrick, P. A. Bean, B. A. Moss, *Biochem. J.* **1995**, *309*, 765; d) B. M. W. Langeveld-Voss, M. P. T. Christiaans, R. A. J. Janssen, E. W. Meijer, *Macromolecules* **1998**, *31*, 6702 – 6704; e) H. Goto, Y. Okamoto, E. Yashima, *Macromolecules* **2002**, *35*, 4590 – 4601; f) G. Qing, X. Shan, W. Chen, Z. Lv, P. Xiong, T. Sun, *Angew. Chem. Int. Ed.* **2014**, *53*, 2124 – 2129; *Angew. Chem.* **2014**, *126*, 2156 – 2161.

[14] R. Lin, H. Zhang, S. H. Li, L. Q. Chen, W. G. Zhang, T. B. Wen, H. Zhang, H. P. Xia, *Chem. Eur. J.* **2011**, *17*, 2420 – 2427.

[15] a) J. M. Ribó, J. Crusats, F. Sagués, J. Claret, R. Rubires, *Science* **2001**, *292*, 2063 – 2066; b) D. B. Amabilino, *Nat. Mater.* **2007**, *6*, 924 – 925.

[16] a) Y. Yan, K. Deng, Z. Yu, Z. Wei, *Angew. Chem. Int. Ed.* **2009**, *48*, 2003 – 2006; *Angew. Chem.* **2009**, *121*, 2037 – 2040; b) Y. Huang, Y. Yan, B. M. Smarsly, Z. Wei, C. F. J. Faul, *J. Mater. Chem.* **2009**, *19*, 2356 – 2362; c) Y. Yan, Z. Yu, Y. W. Huang, W. X. Yuan, Z. X. Wei, *Adv. Mater.* **2007**, *19*, 3353 – 3357; d) R. Oda, I. Huc, M. Schmutz, S. J. Candau, F. C. MacKintosh, *Nature* **1999**, *399*, 566 – 569.

[17] G. F. Liu, W. Ji, W. L. Wang, C. L. Feng, *ACS Appl. Mater. Interfaces* **2015**, *7*, 301 – 307.

[18] S. Zhang, *Nat. Biotechnol.* **2003**, *21*, 1171 – 1178.

Received: October 31, 2015
Published online: December 9, 2015

